Brno University of Technology
Faculty of Civil Engineering
Institute of Structural Mechanics

Doctoral Thesis Statements

Teze dizertační práce

Brno University of Technology
Faculty of Civil Engineering
Institute of Structural Mechanics

PROBABILISTIC DISCRETE MODEL OF CONCRETE FRACTURING

PRAVDĚPODOBNOSTNÍ DISKRÉTNÍ MODEL PORUŠOVÁNÍ BETONU

Ing. Jana Kaděrová

Study Programme: Civil Engineering/Structures and Traffic Constructions

Supervisor: doc. Ing. Jan Eliáš, Ph.D.

Brno 2018

Contents

Introduction

The general focus of researchers in civil engineering is to understand, model and predict behavior of civil engineering structures. Such ability requires to have strong foundations in understanding the behavior of materials used to build these structures. One of the most common material in civil engineering practice is concrete and similar silicate composites.

A significant aspect of the behavior of concrete structures is their nonlinear response to loading which is, moreover, random due to its heterogeneous nature. An accurate model of concrete that would be able to capture the generation and development of microcracks and their subsequent interconnection into macrocracks has therefore to take into the consideration the natural disorder of the inner structure and associated inherent (natural) variability of the local material parameters that lead into the random response of the structural members. The numerical model has to be able also to describe the post-critical behavior of the material with the development of the zones of intensive energy release. Such zones are referred to as the fracture process zones and it is generally agreed that the phenomena defining the member overall strength take place here. Therefore, precise description and understanding of these zones are essential for the modern civil engineering.

Numerical modeling combined with laboratory testing is the most common and most efficient way of detailed investigating of the behavior of materials and members in engineering today. Correct numerical model can provide a strong tool for intensive virtual testing with wide range of possible test setups (sometimes hardly feasible in laboratory) while physical experiments ensure the model validity and correctness. Both methods need to be combined together so that their correctness and applicability can be proven.

The discrete modeling of materials provides several advantages compared to the classical continuum models. They offer a convenient tool for modeling the members made of composites due to their ability to describe the heterogeneous inner structure. At the same time, by implementation of relatively simple formulation of the constitutive relation, they can simulate the phenomenon such as softening of the material in the direction orthogonal to the cracks, etc. Such capability is, on the other hand, the reason for higher computational demand of such models. Despite this fact, discrete material modeling became a well-known method in the modern engineering.

The dissertation thesis deals with the behavior of concrete as a representant of

heterogeneous material with a quasi-brittle response to the mechanical loading. It investigates possibilities of application of a modern computational model of concrete which is capable of capturing the mechanical behavior on the scale of its grains (meso-scale modeling). The model chosen for such study is the *lattice-particle* model which had been developed by G. Cusatis and collaborators [3, 4, 5] under the name LDPM (lattice discrete particle model). It describes the material as an assembly of discrete units. This well-known model has been extended by incorrporation of the spatial variability of selected model parameters [7]. The parameters that have been considered as random are the local tensile strength of the contact between two aggregates and the fracture energy of this bond. These parameters have been defined by means of the mutually correlated random fields. Such an additional source of disorder of the response could help the model to correspond better to the experimental results. The enhanced model could also be able to address the natural localization of damage that appears in the structural models without any strong stress concentrators.

The thesis aims to deliver the robust numerical model combining the probabilistic models with the advanced mechanical model of concrete on its meso-level scale. Such model is employed in an intensive virtual testing of the concrete members with different input conditions. Correct behavior of such numerical model is guaranteed by the validation based on comparison with the real measurement. For that reason, the results of the computational model are compared to some published experiments.

Objectives

- Application of the discrete model enhanced by the spatial variability considered in form of random field

- Identification of the model parameters based on the experimental data from wide series of bent concrete specimens of different sizes and notch depths

- Model validation based on the experimental data

- Study on performance of the basic and enhanced numerical models; evaluation of the response variability and the study on the influence of the autocorrelation length of the random field on the overall member response

- Description and evaluation of the nonlinear zone active during the model loading with the main focus on size and shape of such zone at the peak load

1   State-of-the-Art

Mechanics of fracture and damage of quasibrittle materials such as concrete focuses on the investigation of the crack propagation occurring in a particular zone around the crack tip. This zone (fracture process zone, FPZ) of such materials is characterized by an inelastic phenomena and its size is usually not negligible compared to the structural size. The classical linear elastic fracture mechanics (LEFM) presumes that the FPZ is a very small region (almost a point) but that does not correspond to the FPZ of concrete, unless the structure is extremely large. To study this region, it is necessary to simulate the FPZ of concrete structures directly.

Numerical modeling of concrete response on mechanical loading is a highly developed field. However, due to the highly heterogeneous nature of concrete and its quasibrittle behavior, it is difficult to develop appropriate model that enables the prediction of its response on the mechanical loading. For this purpose, a range of complex numerical models were developed. These models allow to simulate both the pre- and post-critical behavior. During the process of failure, the stress is gradually released in the fracture process zone at the top of the macroscopical crack. This behavior can be attributed to the material heterogeneity. Therefore, it is reasonable to include the heterogeneity directly to the models. Material heterogeneity can be represented in both, the continuum models, and also in the discrete models. The discrete models describe the material as an assembly of mutually connected discrete units. The most simple and also least phenomenological are the classical *lattice models* [13, 22, 14, 23, 16] with brittle-elastic elements and a lattice geometry independent of the inner structure of the material. These models could be computationally inefficient for a simulations of larger concrete members. Significant reduction of the computational time can be achieved by creating the discrete cells around every concrete mineral grain. Such models, often termed the *lattice-particle models*, can be applied for simulation of larger material volumes [1, 3, 15, 7]. The lattice-particle models usually utilize more complex and phenomenological contact behavior between particles as they need to mimic the effects of excluded heterogeneity at lower scale.

One of the advantages of meso-scale models with randomly generated mesostructure is that a large potion of the spatial variability in the local material properties is automatically included. It is because specimens modeled with irregular mesostructure automatically exhibit many features of random quasibrittle behavior. The model offers the possibility to include also an additional material randomness by considering some

3

parameters as random quantities. These random parameters are usually simulated as spatially varying in a form of stationary random field [25, 10, 11]. The probability distribution of random fields representing the local material properties, and also its autocorrelation and cross-correlations (relationships between random variables), need to be defined. The paper presents such an enhanced lattice-particle model and numerical studies performed with it on a three point bent beams with and without notch.

The presented probabilistic meso-scale models have therefore two sources of the variability of results. One comes from the random heterogeneity, and the other from the random fluctuations of parameters. The thesis is aimed to reveal the influence of the spatial fluctuation of the model parameters on mechanical response of the model. The version of the model without the additional random variability in parameters is called here *deterministic model*, whereas the version enhanced by the spatial fluctuation of parameters is referred to as the *probabilistic model*.

2 Discrete Model

2.1 Deterministic discrete model

The discrete model is implemented according to papers of Gianluca Cusatis [5, 6]. Initially, spheres representing mineral grains in concrete are randomly generated inside the volume of the specimen without overlapping. The radii of spheres are sampled using the Fuller curve with maximum diameter 10 mm. Based on the position of spheres and their radii, tessellation is performed and the discrete units associated with the mineral grains are created. The units are treated as ideally rigid and they are interconnected at their contact facets. The connection is realized via three internal forces (one normal and two tangential) that are calculated according to nonlinear constitutive equation. The strains for each direction are obtained from discrete displacement jump at the facet center divided by length of the connection. After the initial elastic regime (with the strength limit dependent on the direction of straining – i.e. by the ratio between normal and tangential strains), an exponential softening is implemented based on a single damage parameter for all three directions. The details about the discrete model can be found in [7].

The discrete model is applied only in areas where crack is expected to initiate and propagate. The rest of the specimen is modeled by linear 8-node finite elements. The connection between the discrete and continuous model is provided by auxiliary grains
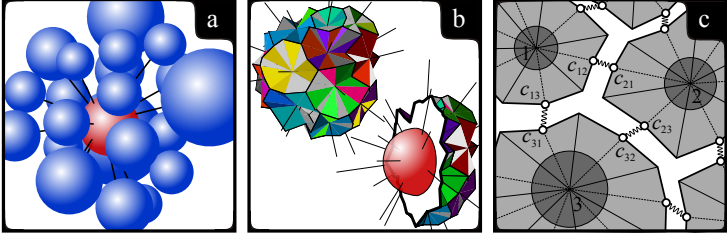
Figure 1: a) Random placement of the grains – simulated meso-structure. b) Rigid cells created by tessellation. c) Contact between adjacent cells. Figure adopted from [7].
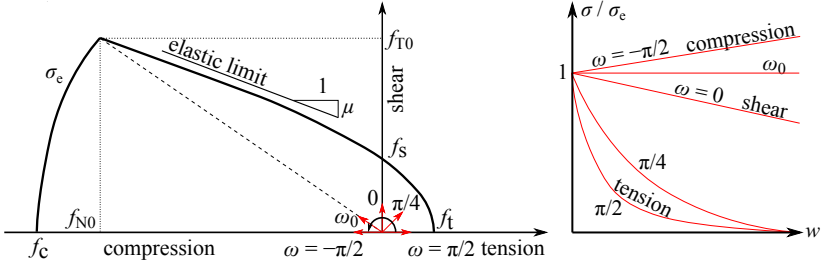

Figure 2: Constitutive law according to [5]: the elastic envelope (right) and the exponential softening (left). Figure adopted from [7].

lying on the boundary surface that are "hanged" on the elements, i.e. their translational degrees of freedom are suppressed and derived directly from the shape functions of the neighboring element.

2.2 Probabilistic discrete model

In the probabilistic extension of the model, it is considered that local tensile-related parameters – the tensile strength, f_t, the shear strength, f_s, the fracture energy in tension G_t and in shear G_s– vary randomly in space. The relationships for the shear properties ($f_s = 3f_s$ and $G_s = 16G_s$ suggested in [5]) are exploited. Therefore, only two parameters, f_t and G_t, are randomized directly. Their spatial variability is assumed in a form of stationary random field. The two spatially varying fields, $f_t(\boldsymbol{x})$ and $G_t(\boldsymbol{x})$, are interrelated and both of them are functions of a single underlying random field $H(\boldsymbol{x})$ defined using a random variable h (characterized via its distribution function) and an autocorrelation function. Entries of the vector $\boldsymbol{x}$ index the spatial coordinates of a point. The stationarity is meant such that the probabilistic distribu-
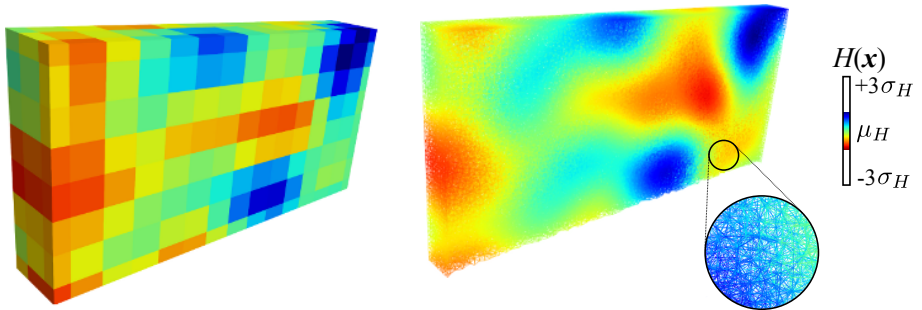
Figure 3: One realization of a random field generated on a regular grid (left) and projected to the model elements (right). Figure adopted from [7].

tion of the underlying random field $H\left(\boldsymbol{x}\right)$ is identical at any point within the domain considered and the autocorrelation function depends solely on the distance of a pair of points, not on their absolute positions.

The h variable has Weibull-Gauss distribution [2, 20, 19] with the mean value $\mathrm{E}[h] = 1$. Based on parameter identification using the experiments [12], its coefficient of variability was estimated to be about 14 % ($\mathrm{CoV}_h = 0.14$).

The autocorrelation of the random fields is given by the following function

$$\rho_{ij} = \exp\left[-\left(\frac{\|\boldsymbol{x}_i - \boldsymbol{x}_j\|}{l_{\mathrm{c}}}\right)^2\right] \tag{1}$$

where l_{c} is the *correlation length*. The random field is generated via series expansion using the EOLE (expansion optimal linear estimation) method [21]. A linear combination of eigenfunctions of the covariance function multiplied by uncorrelated Gaussian random variables are used to perform the series expansion of the random field over grid values using the orthogonal decomposition [24]. The generation of samples of random field becomes extremely computationally demanding for short correlation lengths. Therefore, the separability of the correlation function into individual spatial dimensions has been exploited and the solution of the eigenfunctions has been decomposed into three separate 1D problems along each spatial coordinate, see the appendix of [7].

3 Identification of the Model Parameters

3.1 Experimental data

Model parameters were identified on a set of experimental data form the Université de Pau et des Pays de l'Adour, France, published in [12]. In the experiment, three types of concrete beams with different depth of a notch were tested in three-point bending, each in four different geometrically similar sizes. Deeply-notched beams (notch-to-depth ratio of $\alpha_{\mathsf{a}} = 0.5$, referred as half-notched) are marked with lower case letter a, shallowly-notched beams (notch-to-depth ratio of $\alpha_{\mathsf{b}} = 0.2$, referred as fifth-notched) with a lower case b and unnotched beams with c. The depth of the beams D was 400, 200, 100 and 50 mm, these size groups are marked with capitals A, B, C and D. The length of all beams was $3.5D$, the supports of the loading machine were located $0.5D$ from edges (bending span equals to $S = 2.5D$). All the beams shared the same thickness of $b = 50$ mm, the width of the notch was also kept constant and equal to 3 mm. The scheme of the individual specimen geometry is depicted in Fig. 4 for each size and notch group.

Overall, from 34 tested beams, 13 beams were deeply-notched, 11 shallowly-notched and 10 were unnotched. The authors of [12] provided the results of the bending experiments in a form of a load$-$displacement ($F-\mathrm{CMOD}$, crack-mouth opening displacement) curves and the values of the peak load F_{max}. The mean curve was used for the identification of material model parameters. The two values presented below the group name correspond to the average peak load, F_{max} [kN], and to the average area under the curve, A [kN·mm]. These two values served for the identification of the tensile strength and the fracture energy.

Due to the high demand of the model on the computational power, the discrete model had been used only in regions where the cracks are most probable to appear to save the computational time.

3.2 Parameters identification and model validation

The parameters of the deterministic model were found in the first step. The original model has 12 adjustable parameters, however, only four of them (some of those with a physical meaning) have been been identified: elastic modulus of matrix, E_{c}, tensile strength, f_{t}, fracture energy in tension, G_{t}, and the parameter α determining the

macroscopic Poisson ratio. The value of the remaining parameters was either calculated using the relation to the other parameters or taken from [5].

The deterministic parameters (tensile strength, f_t, and fracture energy in tension, G_t) have been identified with help of only a part of the experimental data – the three largest sizes of beams with a deep and a shallow notch (groups Aa, Ba, Ca, Ab, Bb, Cb). The rest of the experimental data served for the validation of the model.
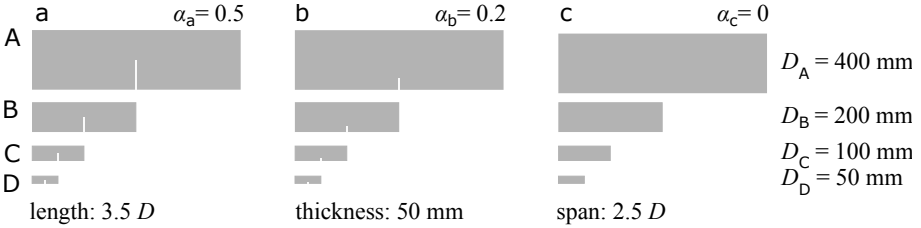

Figure 4: Schematic overview of beam geometries tested in [12].

Once the deterministic model parameters have been found, the parameters of the probabilistic extension could be identified. To simulate of the loading capacity of a quasi-brittle solid, the material strength and the fracture energy can be considered as the most important parameters. Therefore, the spatial variability of these two parameters was taken into account when simulating the fracture process by the probabilistic model. Here, the tensile strength of the material, and the tensile fracture energy, are considered to be linearly dependent on the random field value, [10]. As an identical probability distribution and coefficient of variation have been used for all these parameters, a single random field could be used to generate values for both parameters.

The chosen distribution F_H (Gauss distribution with the Weibullian left-hand tail) is defined by four parameters of the distribution. To find one of them based on the experimental results – the coefficient of variation of the random field H (the other two parameters, m and p_{gr} were set according to literature and $\mu = 1$), the following assumption was exploited: if the strong stress concentrator is present, the influence of the spatial variability (correlation function) on the mean strength is negligible, as was shown in [8, 9]. The strength of the beams with a deep notch is dependent mostly on the material in the closest neighborhood of the notch tip, which is defined only by the probability distribution F_H. By introducing a strong stress concentrator, the influence of the correlation length becomes negligible and only the local properties of the random field (distribution F_H) matters. Therefore, the results from the tests on deeply-notched beams were used to determine CoV.

Coefficient of variation was identified from the results of the second largest beams with a deep notch (group Ba) as it had the highes population number of tested specimens. The minimum error (the difference in CoV between the experimental results and the simulated responses from the probabilistic model with the infinite correlation length) has been searched in an iterative procedure. Based on such optimization process, the CoV of F_H was estimated to be 0.14. Knowing the value of CoV, the correlation length, l_c, could be roughly estimated by matching the peak loads from experiments on unnotched beams, where the mean peak load strongly depends on the correlation length, as shown in [8, 9]. The value of correlation length of the random field of strength and fracture energy was estimated from the largest unnotched specimens (group Ac) to match the average peak load from experiments. The resulting estimate was $l_c = 0.1$ m.

Once the model parameters were identified, the performance of the model (deterministic and probabilistic) could be validated [17]. Ten simulations with the deterministic model were performed for each of the specimen type and size. The curves simulated by the deterministic model are in a good agreement with the experimental results. The model can predict the peak load as well as the post-critical part of loading. Although the model is deterministic (with constant parameters for all ten simulations), its response is scattered. The reason is the random location and size of grains which is different for each simulation. Yet, the scatter of deterministic model is still not sufficient when compared to the experimental one. It is therefore believed that another source of disorder should be added to simulate more realistic response of concrete specimens. Such a source can be the random spatial fluctuation of parameters in form of a random field.

With the probabilistic discrete model which contains both sources of material disorder (the heterogeneous random inner structure and the spatially fluctuating random material parameters), 24 simulations of each test setup were performed. Again, the simulated responses are in good agreement with the experimental results. Comparing both types of simulations, it is obvious that after introducing the variability of the input parameters, the scatter in the maximum load as well as in the dissipated energy increased for the notched beams, while the mean value of the maximum force remained unchanged. For the unnotched beams, besides the increase of the response scatter, the decrease in the average maximum force is present. The random field helps the inelastic strain to localize into macrocracks. Examples of two different beams simulated by the probabilistic model can be seen in Fig. 5: one deeply-notched beam (Aa) of the
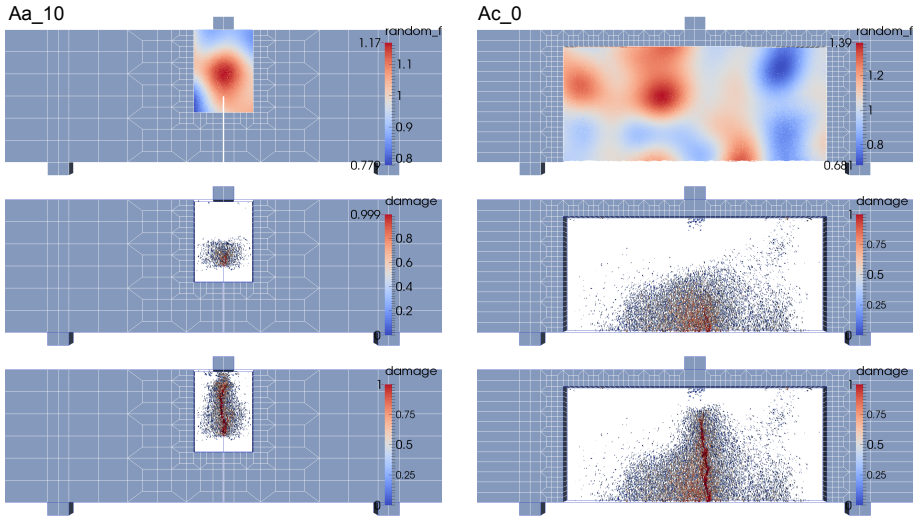
Figure 5: Examples of two probabilistic simulations. Left: deeply-notched beam Aa. Right: unnotched beam Ac. First row: realization of the random field H used in the simulation; second row: damage parameter at the peak load; third row: damage parameter at the end of the simulation.

largest size and one unnotched beam of the largest size (Ac), both with their random field H used for the scaling of strength and fracture energy (the first row), the damage parameter at the peak load (the second row) and the damage parameter at the end of the simulation (the third row). The figure nicely illustrates the localization of damage at the peak load and macrocrack formed at the end of the simulation.

4   Influence of the Correlation Length

4.1   Determining the correlation length and scaling of fracture energy

The correlation length, l_c, has been roughly estimated in the first step by matching the maximum load on the largest unnotched beams. Nevertheless, it is interesting to investigate how the changing value of l_c influences the simulations. Therefore, an effect of changing l_c on the overall response has been investigated.
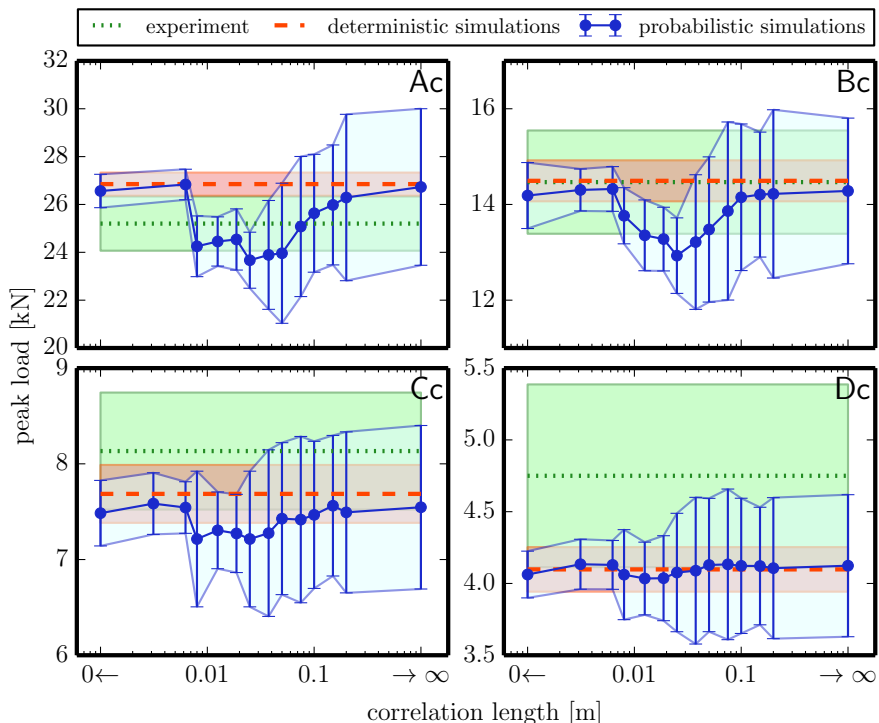
Figure 6: Experimental (green), deterministic (red) and probabilistic (blue) peak load [kN] vs. correlation length [m] of the random field from simulations of all sizes of unnotched beams (groups Ac, Bc, Cc, Dc).

A set of 24 probabilistic simulations was calculated for each size of deeply-notched (groups a) and unnotched (groups c) beams, repeatedly for different values of l_c. The correlation length varied between "zero" and infinity (overall 14 values of l_c have been considered). The zero correlation length refers to the probabilistic setup where each contact between particles has independent random value of h, yet all the values are sampled from the same probability distribution F_H. For the infinitely large correlation length, the random field $H(\boldsymbol{x})$ degenerates into a single constant (which is random for each simulation) value h in all its points – simulation with such a field is identical to the deterministic simulation with parameters multiplied by h. Figure 6 presents the dependency using 24 unnotched simulations in each size group. It can be observed that simulations with different values of l_c did not provide the same mean
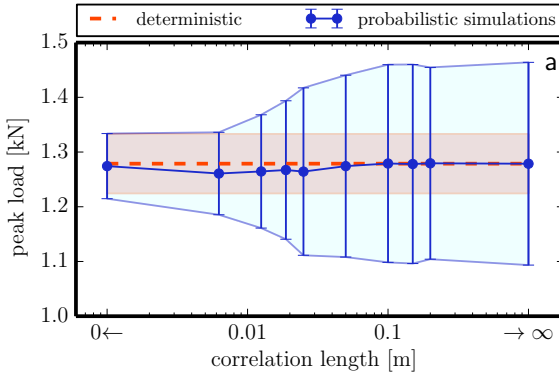
Figure 7: Dependency of the maximum load on the correlation length l_c of the random field for deeply-notched beams (type a).

peak load. Contrary to the unnotched beams, the average peak load of the notched beams is not influenced by the correlation length l_c. The standard deviation of the peak load seems to be increasing with the value of l_c. Surprisingly, the mean peak load from the probabilistic model did not reach the mean load of the deterministic model. This fact was caused by the scaling method used to sample the fracture energy. In these simulations, the linear scaling of fracture energy was applied which results in nonlinear relation between strength of the probabilistic model with $l_c = \infty$ and the applied scaling factor h.

For the further simulations, the scaling method was changed: the tensile strength remains a linear function of the random field H, but the fracture energy has quadratic dependence on H. Such a nonlinear relationship between f_t and G_t has the advantage of preserving the character of the material (ductility vs. brittleness). As a consequence, the peak loads of the whole structure are proportional to the value of h.

4.2 New geometry

To investigate the relation between the structural strength and the correlation length, a new (more convenient) geometry of the concrete beams is introduced. In this new simulation series, three types of beams are tested again: deeply-notched (half-notched, marked a), shallowly-notched (fifth-notched, marked b) and unnotched beams (marked c). The model parameters have been adopted from the simulations of the bending experiments [12].
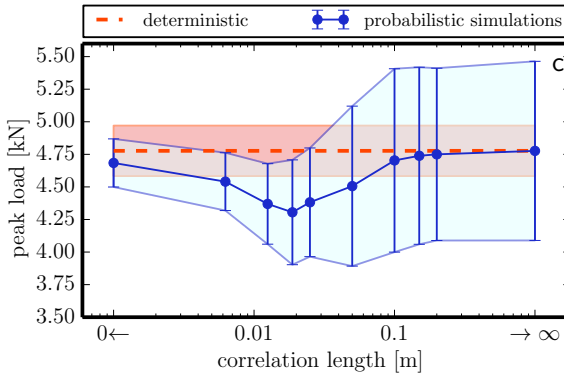
Figure 8: Dependency of the maximum load on the correlation length l_c of the random field for unnotched beams (type c).

Obtained dependency of the mean maximum load on the correlation length is plotted in Figs. 8 and 7. The blue error-bars show the probabilistic models differing in l_c whereas the red line and the shaded areas show the mean $\pm$ one standard deviation calculated from the peak loads of 100 deterministic simulations. In the graphs, we can observe some common phenomena.

In the case of infinite correlation length, $l_c = \infty$, the dependence on a spatial coordinate $\boldsymbol{x}$ vanishes and the random field is defined by a single random variable, $H(\boldsymbol{x}) = h$. Therefore, the samples of the random field are random constants over the specimen domain. This case corresponds to the deterministic simulations with variable multiples of fracture parameters $f_t = \overline{f_t}h$ and $G_t = \overline{G_t}h^2$. The source of disorder in each simulation is then from the inner structure only. In the thesis, the derivation of the variation coefficient of the model with $l_c = \infty$ is derived.

In the other limit, $l_c = 0$, the random field is just a theoretical construct. This case is modeled by assigning each contact (facet) in the discrete model a random value of h independently of the surrounding contacts. Nevertheless, the mean and standard deviation from probabilistic simulations approximately equal to the mean and standard deviation from deterministic simulations. This can be observed for all three beams geometries (notched and unnotched beams).

For the values of the correlation length lying in between zero and infinity, notched and unnotched beams behave in a different manner: the notched beams do not show a sensitivity to the value of the correlation length of the random field and their prob-
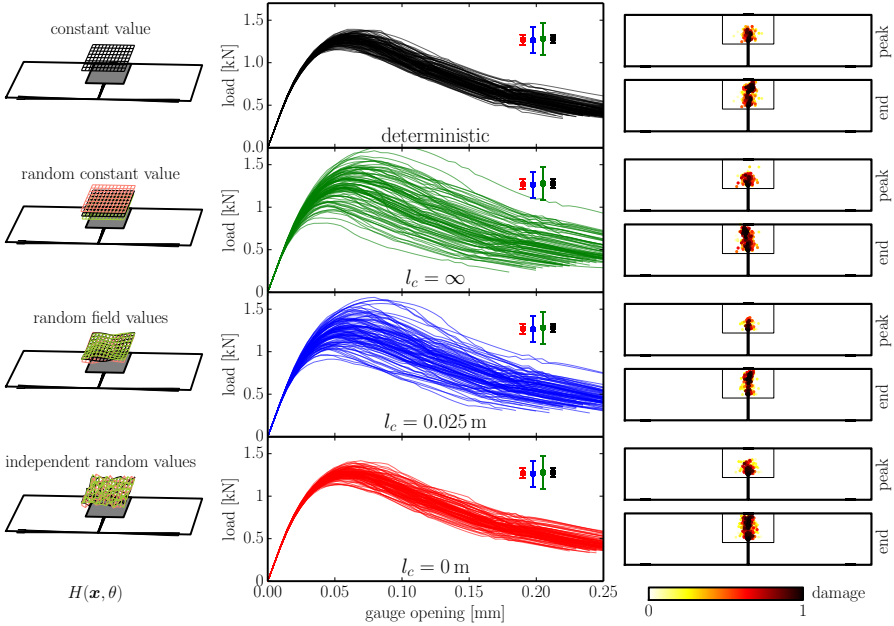
13

Figure 9: Notched beams. Left: Schematic representation of spatial variability of $H(\boldsymbol{x})$. Middle: load – gauge opening curves for selected values of l_c. Right: Damage pattern at the peak load and at the end of one simulation.

abilistic mean strength follow the value of the deterministic simulations. For the un-notched beams, some reduction of the probabilistic mean strength can be observed.

The results of probabilistic and deterministic simulations are also presented in Fig. 9 for deeply-notched beams and in Fig. 10 for unnotched beams: the deterministic simulations (the first row) and the probabilistic simulations with l_c equal to ∞, 0.025 m and 0.

By comparing the deterministic and the probabilistic simulations, it can be observed that the incorporation of the spatial variability in the parameters leads, for the beams with a notch, to an increase in variance of the peak load while the mean values remain unchanged. The reason for such a behavior is presence of the stress concentrator at the tip of the notch. The crack is forced to start from the notch and therefore the maximum load is dictated by the small volume of the material above the notch tip only. The amount of this critical volume is determined by the material internal length and it can be assumed approximately constant for any randomness applied.
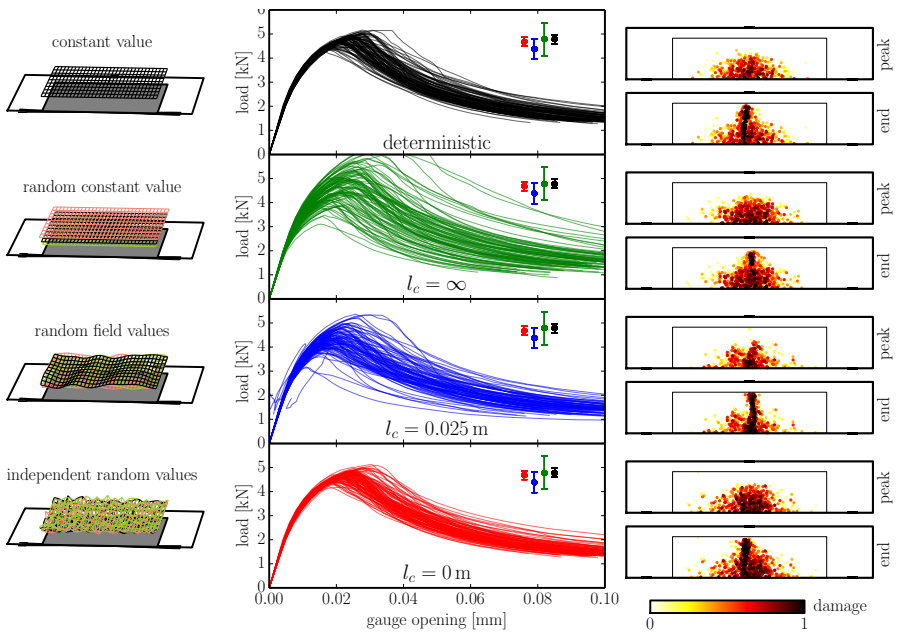
14

Figure 10: Unnotched beams. Left: Schematic representation of spatial variability of $H(\boldsymbol{x})$. Middle: load – gauge opening curves for selected values of l_{c}. Right: Damage pattern at the peak load and at the end of one simulation.

The shorter the correlation length, the more spatial fluctuations of material properties are present inside this volume. However, the crack initiating there has to (at least partially) damage most of the bonds inside that critical volume and the strength is dictated by almost all the values of h there. Some kind of averaging of these fluctuations is therefore present. The averaging inside the critical volume leads to the decrease in standard deviation of the peak load as the correlation length decreases. In the limit case of $l_{\mathrm{c}} = 0$, the averaging is so strong that the standard deviation is about the same as in the deterministic simulations, i.e. the randomness due to spatial fluctuation completely diminishes; the variability in parameters due to random h is eclipsed by the effect of random orientation and size of the facets.

For the unnotched beams, the situation is quite different. The absence of stress concentrator allows the cracks to choose where to initiate from and where the critical cluster of damage occurs. Therefore, such a critical volume can be selected anywhere along the bottom surface. It will naturally choose the worst combination of stress

and strength. The strength is again given by averaging the fluctuations within the critical volume (and of course by the grain arrangement there). As the correlation length decreases, the rate of fluctuations increases and the probability that some weak area occurs and allows the crack to initiate increases as well. Therefore, the mean strength decreases with decreasing l_c. However, there is a limit dictated by the size of the critical volume. When the random field H starts to fluctuate inside the critical volume too much, the averaging effect leads to an increase in the strength of the critical volume. The more fluctuations within the critical volume, the stronger the averaging. In a limit case of extremely small $l_c \rightarrow 0$, the randomness has no effect and the mean of the peak load should be equal to the mean peak load from the deterministic simulations [18].

Now, a closer look at the spatial distribution of the energy dissipation inside this active zone can be taken. The following section will deal with several attitudes how to evaluate and describe the active zone and its energy release.

5   Spatial Distribution of Energy Dissipation

This chapter of the thesis is focused on the region created during the fracture process in the discrete model where the most of the damage and the energy release take place. Such zone of the material is usually referred to as a fracture process zone (FPZ). The ability to provide information about the FPZ is limited to detailed meso-level models. The meso-level discrete model used in this work enables tracing the process of formation and growth of the FPZ and subsequently also describing its size and shape in different phases of the loading. The FPZ also changes if we employ the spatial variability (the random field of strength and other parameters), as well as the test setup (notched and unnotched geometry) [7].

The data obtained during the virtual experiment on three-point bent beams was used to investigate the active zone. The same hundred simulations from previous chapter with the deterministic and probabilistic model (for every value of the correlation length of the random field) were used.

To process and evaluate the data from simulations, several strategies are used: applying a mesh grid and evaluating the information on each cell of the grid (i); approximating the active zone shape with various geometrical shapes (ii); and using the outlier and novelty detection tool in Python (iii).
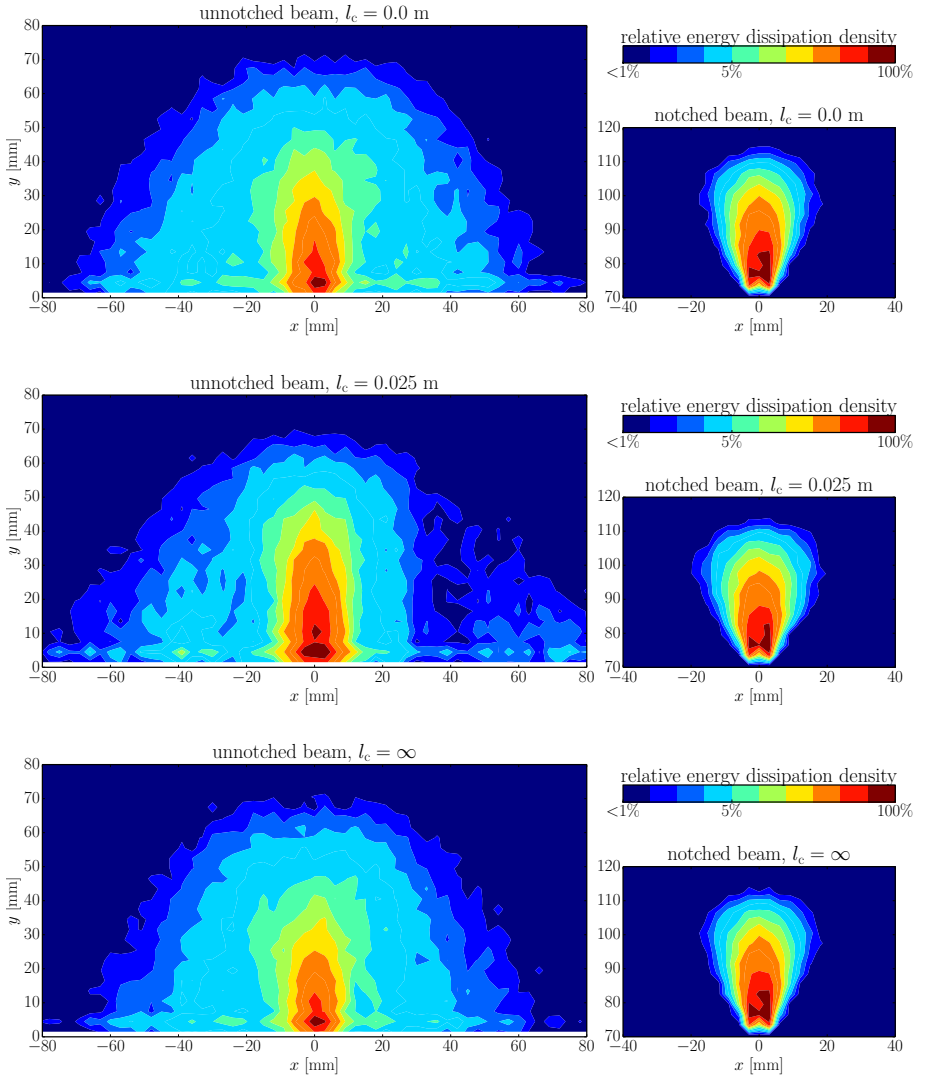
Figure 11: Mesh grid evaluation of the active zone: contour plot of $\bar{R}_b$ (normalized relative dissipated energy) in bins for three different models.

5.1 Mesh Grid Procedure

In the mesh grid method, the beam is divided into regular orthogonal grid with a defined cell size and each contact is assigned based on its coordinates to the appropriate grid cell. Then, the observed quantity is summed up inside each cell and the results can be presented. The mesh grid was considered as two-dimensional (each cell has the same thickness as the beam). The results can be plotted for different phases of the loading (elastic regime, peak, postpeak). For the investigation of the active zone, we will focus now on the peak of the loading curve, when the beam is loaded by the maximum force. For this purpose, we are not interested in the total energy released from the beginning of the test till the peak load but only in the one time step when the peak load is reached. This allows us to investigate the rate of energy release at the peak load.

Figure 11 shows the normalized dissipated energy $\bar{R}_b$ of the mesh grid bins on the three different probabilistic models of unnotched (left) and notched (right) beams. The relative dissipated energy R_b of each bin was normalized with respect to the bin with the highest value – the dark red color represents the bins with the highest relative dissipated energy while the dark blue corresponds to the regions with energy below 1 % of the highest value. Comparing the active zones of the notched and unnotched beams, it can be observed that, for unnotched beams, the region with a low energy dissipation ($\bar{R}_b \in \langle 1\%, 5\% \rangle$) is much larger than in case of the notched beams. The damage and energy release happen, in case of unnotched beams, in much larger portion of the beam. On the contrary, region of high energy dissipation is quite similar, both in size and shape. When comparing the active zone of different correlation lengths, it seems that there is no influence in notched case, but some in unnotched case.

Contour plots were evaluated for each of the correlation length l_c. Three contours in elevation corresponding to approx. 20 % (solid line), 40 % (dash line) and 60 % (dotted line) of the maximum $\bar{R}_b$ are plotted in Fig. 12, both for unnotched beams (top) and notched beams (bottom). Top three diagrams always show the maximum width of the zone (left), its maximum depth (middle) and the square root of the overall area (right) enclosed by the selected contour. The horizontal lines in these plots represent the results of corresponding deterministic model. From these diagrams, the dependence of the shape of the active zone on the correlation length of the random field can be clearly observed.

Looking at the diagrams of the unnotched beams (Fig. 12a), a strong influence
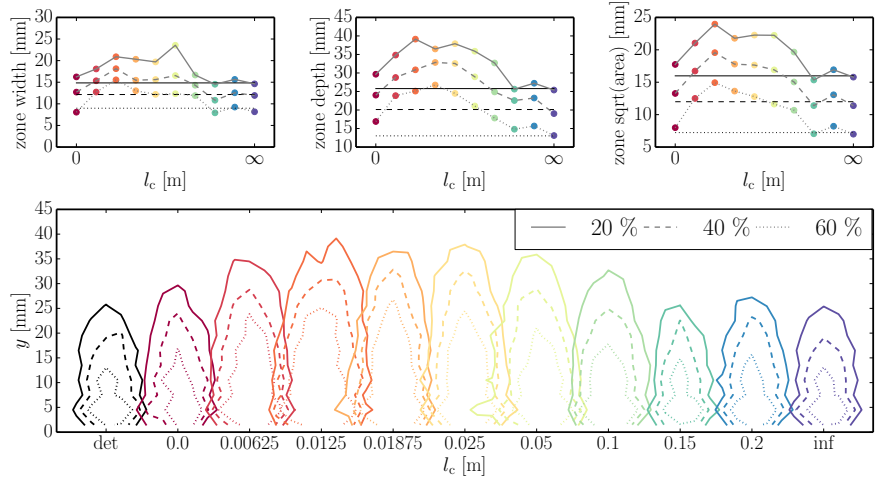
(a) Unnotched beams
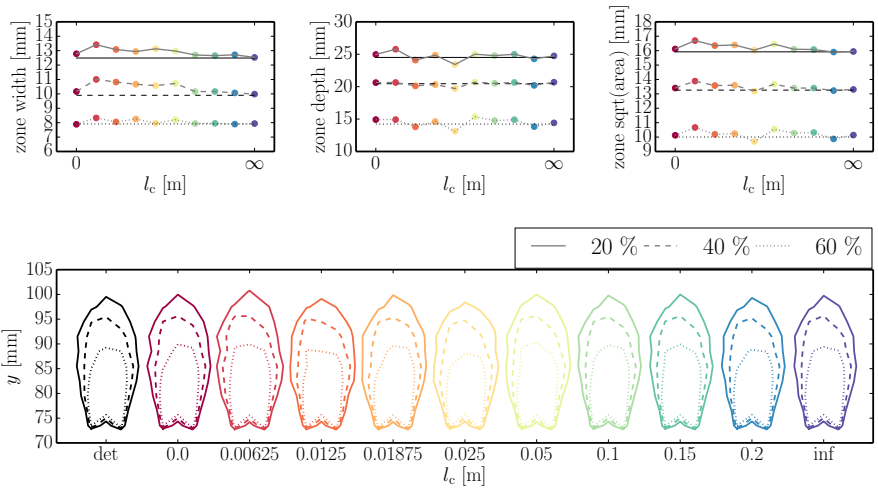
(b) Notched beams

Figure 12: Mesh grid evaluation of the active zone: Three selected contours and their dependence on width, depth, area and shape on the correlation length.

of the correlation length on the size of the active zone can be seen. For the value of $l_c = 0.0125$ m, the active zone reaches the largest area. With growing or reducing value of l_c, the zone gets smaller. In extremes ($l_c = \infty$ and $l_c = 0$), the zone has approximately the same size. For the deeply-notched beams, the active zone seems to have no dependence on the random field and its correlation length. This is shown in all three top diagrams of Fig. 12b – the zone width, depth and area are constant over all the values of l_c.

5.2 Approximation of Active Zone by Geometrical Shapes

Another way how the shape of the active zone can be displayed is to find the geometrical shape which encloses as much of the specified quantity as possible (generally, it can be energy or damage but due to reasons mentioned in the thesis, relative energy difference at the peak was considered). In this procedure, a chosen geometrical shape of a small size was placed to the point of high stress concentration (the notch/crack tip) and then the energy dissipated inside the region was calculated. Different geometrical shapes were used: rectangle, half-ellipse and half-circle with different width-to-depth ratio (for unnotched beams) and ellipse and rectangle (for notched beams).

Subsequently, the region was scaled by a given constant (Fig. 13) and the relative energy $\Delta \bar{E}_A^{(p)}$ inside the region A was summed up again. The sum of the overall relative energy is equal 1.

In following graphs, the dependence of the portion of dissipated energy (the ratio between the energy inside the region defined by the geometrical shape $\Delta \bar{E}_A^{(p)}$ to the total released energy $\Delta \bar{E}^{(p)}$ over the whole beam) inside the region of area A is presented. The average curve was found for each of the geometrical shape. These curves are presented in Fig. 14 for unnotched beams and in Fig. 15 for notched beams. Again, the results of the deterministic and three probabilistic models differing in their correlation lengths are plotted.

According to the assumption, the geometrical shape which reaches the certain level of $\Delta \bar{E}_A^{(p)}$ with the smallest area has the most optimal shape for the approximation of
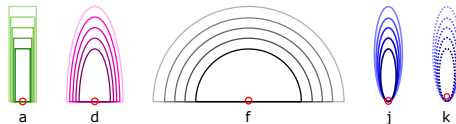

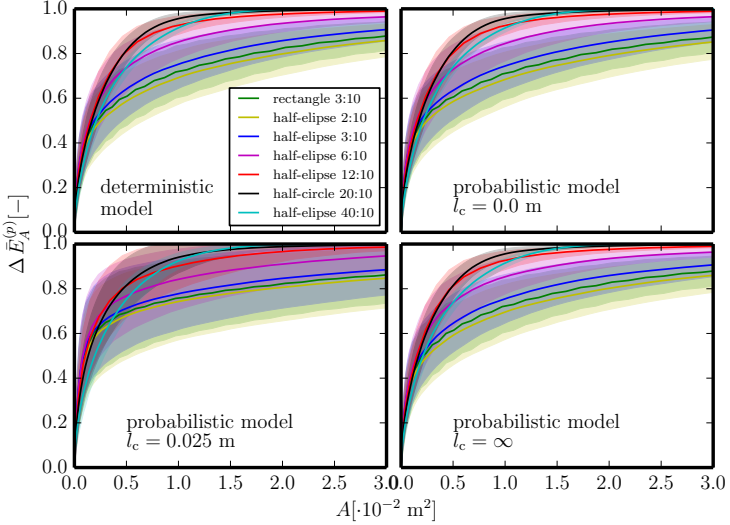Figure 13: Examples of scaling of the selected geometrical shapes.

Figure 14: Portion of the relative energy included in different geometrical shapes vs. their area (unnotched beams).

the active zone. If we look at the results, different shapes satisfy this assumption for different values of $\Delta \bar{E}_A^{(p)}$, nevertheless the results are similar for all four models.

Let us now focus on the results for the unnotched beams in Fig. 14. In the initial part of the diagrams, the purple curve corresponding to the half-elliptical shape (d) with width-to-depth ratio of 6:10 performs the best. It wins up to 50 % of the total energy (for the probabilistic model with $l_c = 0.025$ m it is even till about 70 %). At that point, the wider shape of the red half-ellipse 12:10 (e) starts to be more convenient till about 80 % of the overall released energy of all simulations $E_{\text{tot}} = \sum_{\text{sim}} \sum_h \Delta E_h^{(p)}$ (for the probabilistic model with $l_c = 0$ about 70 %). Above this level, the black curve of the half-circle (f) 20:10 becomes the top one till the very last part (about 98 %). The remaining 2 % of the total energy are again in some wider region, therefore the widest cyan half-ellipse (g) 40:10 works the best in the final stage around 100 % of the overall $\Delta \bar{E}^{(p)}$.

For the notched beams, the most convenient shape seems to be the rectangle (i) with width-to-depth ratio of 5:10 which is marked with the dark green color. For all four models, this shape is the best approximation till the threshold of about 95 % of the total energy. Above this limit, the wider ellipse B 6:10 (m) shifted 5 mm downwards from the notch tip seems to approximate the shape of the active zone the best.
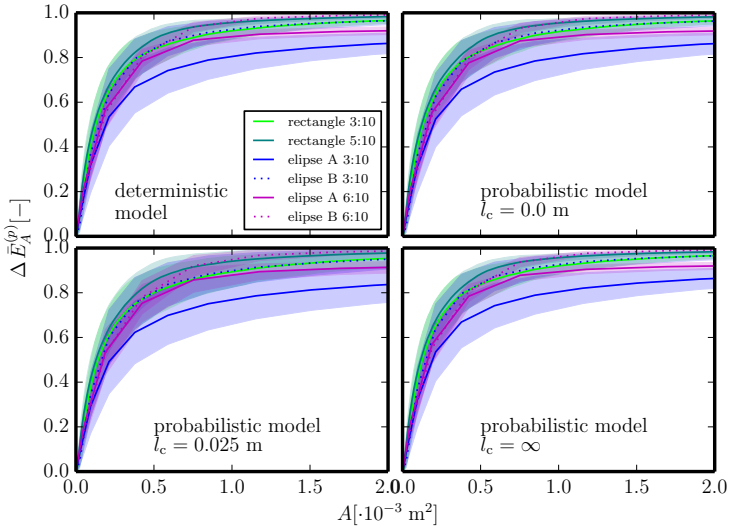
Figure 15: Portion of included relative energy in different geometrical shapes vs. their area (notched beams).

5.3 Novelty Detection Tool

The third method used to find and describe the active zone at the top of the loading curve was the use of `scikit-learn` (machine learning tool) in Python (built on NumPy, SciPy, and matplotlib). This package contains a simple and efficient tools for data mining and data analysis, it is open source, commercially usable (BSD license), and reusable in various contexts. We used the outlier and novelty detection procedure to find an area of the active zone where the most of the fracture energy releases during the peak step. Practically, we let the procedure find the best area with defined amount of the observed quantity (the relative dissipated energy).

Figures 16 and 17 show two results of the analysis by the novelty detection tool in Python. Only one example of deeply-notched and unnotched beams is presented – simulations by probabilistic model with the correlation length of $l_c = 0.025$ m.

For the notched beams (Fig. 16), the active zone is concentrated within a relatively small area above the stress concentrator (the notch). Therefore, the Python tool was able to find all the contours from 10 % (red line) up to 90 % (dark blue line) and they are still close to the notch tip and have a simple shape. On the contrary for the unnotched beams (Fig. 17) only some contours were evaluated (from 10 to 50 %). The
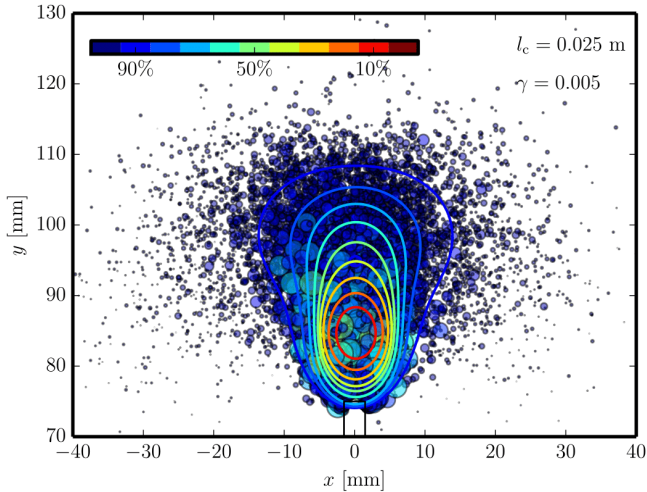
Figure 16: Notched beams: Relative energy dissipated at individual contacts and border contours specifying the amount of the dissipated energy (outlier and novelty detection tool).

active zone here is spread into a larger area around the final crack position as visible from the blue circles in the figure background. However, the most of the energy is released in a small region around the macrocrack location and is bordered by the red line in the figure. The turquoise contour corresponding to the 50 % of the overall dissipated energy already defines an area which is not compact any more. For the higher contours (above fifty procent), the outlier and novelty detection tool is not able to find a region that would be compact but is divided into several regions. Due to this reason, the higher contours are not plotted in the figure.

If we focus now on the shape of the active zone defined by the calculated contours, we can see that for the notched beams, it changes from an oval shape bordering the center of the active zone (red curve) to an upturned pear shape (the dark blue line) of the zone with almost all the dissipated energy. The region with the 50 % of the overall dissipated energy is about 10 mm wide and 22 mm deep (turquoise line). For the unnotched beams, the zone looks quite different: the red contour is pear shaped and the zone grows more in the vertical direction (the contours up to 40 % are elongated), the last plotted contour shows that the zone would have further on an oblong shape. The 50% contour has approx. 35 mm in width and 45 mm in depth.
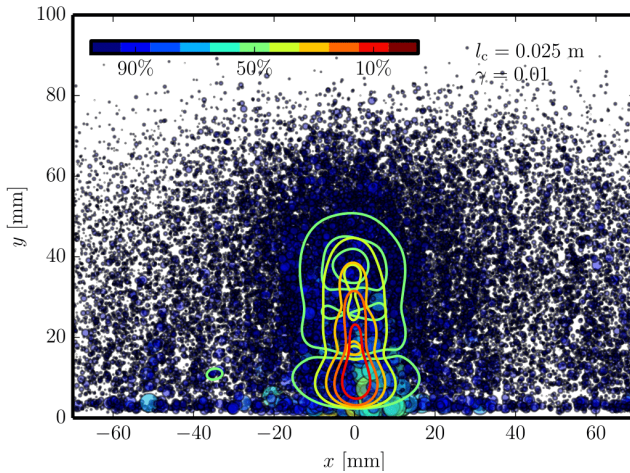
Figure 17: Unnotched beams: Relative energy dissipated at individual contacts and border contours specifying the amount of the dissipated energy (outlier and novelty detection tool).

6 Conclusion

The presented thesis aimed to validate an advanced numerical model of concrete and to investigate and describe, with the help of the validated model, the fracture process inside the concrete members subjected to mechanical loading.

The discrete model was adapted and extended with the spatial variability of parameters in form of random field. The model in its basic and extended form was validated based on the experimental results on beams of different size and configuration of the stress concentrator loaded in three-point bending test.

Two versions of the model were used: the basic (deterministic) one with the random arrangement of the particles representing the random inner structure of the material and the extended (probabilistic) one introducing an additional source of variability into the model – the random material parameters defined in form of the random field. Such an extension aims to improve the response of the model regarding its variability so that it better corresponds to the real data measured in the laboratory. For the deterministic model, the elementary static and kinematic relations are introduced as well as the procedure of generation of the topology of the model. For the probabilistic model, the process of generation of the random fields is briefly described.

The parameters of the introduced versions of the model are identified based on the laboratory experiments from literature. Three different test setups of bended beams were tested (deeply-notched, shallowly-notched and unnotched beams) in four different sizes. With the validated model, a wide series of numerical experiments was simulated. The influence of the correlation length on the peak load of the probabilistic model was studied.

A new series of simulations was designed with a focus on its convenience for the study of the mentioned dependence. Again, three different setups (deeply-notched, shallowly-notched and unnotched beams) were loaded in three-point bending test. The response was simulated in the same manner: with the deterministic model and also with the probabilistic one with ten different values of the correlation length (varying between zero and infinity).

The results of the new series revealed the following phenomenon: regarding unnotched beams, the strength evinces a drop around a certain value of the correlation length. For a given setup, the value was around 19 mm. In such case, the zone of the lower random local strength corresponds approximately to the size of the zone that has to be damaged so that the overall failure happens. If the correlation length is changed towards lower values (zero) or higher values (infinity), the mean probabilistic strength matches again the deterministic value. This can be explained by the fact that for the infinitely high value of correlation length, the random field has a constant value in all its points. This value is different for each simulation, however, their average corresponds to the value of the deterministic model. On the other hand, a random field with a zero correlation length has a different value in each of its point. To reach the failure, it is necessary that the material is damaged in a certain volume and the different local point values are again averaged in this region. Therefore, the deterministic average is reached again.

For the notched beam setup (deeply as well as shallowly), such trend is not observed. In this case, the path of the crack is more or less known in advance as it is dictated by the notch. Therefore, the local strength at the top of the notch tip does not play an important role and the average peak strength can be considered as equal for any correlation length of the random field (although, a slight drop can be observed for values around $l_c = 6$ mm.)

Finally, the thesis describes the energy release and the region in which it takes place. Three different approaches were suggested, evaluated and compared. In the first one, the beam was spatially divided into regular orthogonal grid and the released

energy was summed up over the facets in each particular cell of the grid. In the second suggested method, the zone active during the testing was approximated with different geometrical shapes (rectangles, ellipses, half-ellipses, half-circles) so that the region can be described in terms of its shape. For the last method of describing the active zone with the highest energy release, the `scikit-learn` package (based on machine learning procedure) implemented in Python was employed. The novelty detection tool looks for the region corresponding to the most intensive occurrence of target event (in our case the released fracture energy).

The above mentioned results gave more detailed insight into the shape and size of the region with the intensive energy release (active zone) as well as its development during the loading. The zone is not constant but its shape and size depend on the phase during the test and also they are influenced by other factors: the geometrical setup of the specimen (notched/unnotched configuration) or the rate of spatial fluctuation of the material parameters.

Bibliography

[1] Bažant, Z.; Tabbara, M.; Kazemi, M.; et al.: Random Particle Model for Fracture of Aggregate or Fiber Composites. *Journal of the Engineering Mechanics Division ASCE*, volume 116, nr. 8, 1990: pages 1686–1705, ISSN 0733-9399.

[2] Bažant, Z. P.; Pang, S.-D.: Activation energy based extreme value statistics and size effect in brittle and quasibrittle fracture. *Journal of the Mechanics and Physics of Solids*, volume 55, nr. 1, 2007: pages 91–131, ISSN 0022-5096.

[3] Cusatis, G.; Bažant, Z. P.; Cedolin, L.: Confinement-Shear Lattice Model for Concrete Damage in Tension and Compression: I. Theory. *Journal of the Engineering Mechanics Division ASCE*, volume 129, nr. 12, 2003: pages 1439–1448, ISSN 0733-9399.

[4] Cusatis, G.; Bažant, Z. P.; Cedolin, L.: Confinement-shear lattice CSL model for fracture propagation in concrete. *Computer Methods in Applied Mechanics and Engineering*, volume 195, nr. 52, 2006: pages 7154–7171, ISSN 0045-7825.

[5] Cusatis, G.; Cedolin, L.: Two-scale study of concrete fracturing behavior. *Engineering Fracture Mechanics*, volume 74, nr. 1–2, 2007: pages 3–17, ISSN 0013-7944.

[6] Cusatis, G.; Pelessone, D.; Mencarelli, A.: Lattice Discrete Particle Model (LDPM) for failure behavior of concrete. I: Theory. *Cement and Concrete Composites*, volume 33, nr. 9, 2011: pages 881–890, ISSN 0958-9465.

[7] Eliáš, J.; Vořechovský, M.; Skoček, J.; et al.: Stochastic discrete meso-scale simulations of concrete fracture: Comparison to experimental data. *Engineering Fracture Mechanics*, volume 135, 2015: pages 1–16, ISSN 0013-7944.

[8] Eliáš, J.; Vořechovský, M.; Bažant, Z. P.: Stochastic lattice simulations of flexural failure in concrete beams. In *8th International Conference on Fracture Mechanics of Concrete and Concrete Structures - FraMCoS-8*, edited by G. R. e. a. Van Mier, Toledo, Spain, 2013, pg. 12.

[9] Eliáš, J.; Vořechovský, M.; Le, J.-L.: Lattice Modeling of Concrete Fracture Including Material Spatial Randomness. *Engineering Mechanics*, volume 5, 2013: pages 413–426, ISSN 1802-1484.

[10] Grassl, P.; Bažant, Z. P.: Random lattice-particle simulation of statistical size effect in quasi-brittle structures failing at crack initiation. *Journal of the Engineering Mechanics Division ASCE*, volume 135, 2009: pages 85–92, ISSN 0733-9399.

[11] Grassl, P.; Grégoire, D.; Solano, L. R.; et al.: Meso-scale modelling of the size effect on the fracture process zone of concrete. *International Journal of Solids and Structures*, volume 49, nr. 43, 2013: pages 1818–1827, ISSN 0020-7683.

[12] Grégoire, D.; Rojas-Solano, L.; Pijaudier-Cabot, G.: Failure and size effect for notched and unnotched concrete beams. *International Journal for Numerical and Analytical Methods in Geomechanics*, volume 37, nr. 10, 2013: pages 1434–1452, ISSN 1096-9853.

[13] Herrmann, H.; Hansen, A.; Roux, S.: Fracture of disordered, elastic lattices in two dimensions. *Physical Review B*, volume 39, nr. 1, 1989: pages 637–648, ISSN 1098-0121.

[14] Ince, R.; Arslan, A.; Karihaloo, B.: Lattice modelling of size effect in concrete strength. *Engineering Fracture Mechanics*, volume 70, nr. 16, 2003: pages 2307–2320, ISSN 0013-7944, size-scale effects.

[15] Jirásek, M.; Bažant, Z.: Macroscopic fracture characteristics of random particle systems. *International Journal of Fracture*, volume 69, nr. 3, 1995: pages 201–228, ISSN 0376-9429.

[16] Jivkov, A. P.; Engelberg, D. L.; Stein, R.; et al.: Pore space and brittle damage evolution in concrete. *Engineering Fracture Mechanics*, volume 110, nr. 0, 2013:

pages 378–395, ISSN 0013-7944.

[17] Kaděrová, J.; Eliáš, J.: Simulations of bending experiments of concrete beams by stochastic discrete model. In *Key Engineering Materials*, volume 627, edited by F. A. M. Alfaiate J., Trans Tech Publications, 2014, ISBN 978-3-03835-235-8, ISSN 10139826, pages 457–460.

[18] Kaděrová, J.; Eliáš, J.; Vořechovský, M.: The Influence of Correlation Length on the Strength of Stochastic Discrete Models. In *Proceedings of the Fifteenth International Conference on Civil, Structural and Environmental Engineering Computing*, number 108 in Civil-Comp Proceedings, Civil–Comp Press, 2015, ISBN 978-1-905088-63-8, ISSN 1759-3433, pages 1–13.

[19] Le, J.-L.; Bažant, Z. P.: Unified nano-mechanics based probabilistic theory of quasibrittle and brittle structures: II. Fatigue crack growth, lifetime and scaling. *Journal of the Mechanics and Physics of Solids*, volume 59, 2011: pages 1322–1337, ISSN 0022-5096.

[20] Le, J.-L.; Bažant, Z. P.; Bazant, M. Z.: Unified nano-mechanics based probabilistic theory of quasibrittle and brittle structures: I. Strength, static crack growth, lifetime and scaling. *Journal of the Mechanics and Physics of Solids*, volume 59, nr. 7, 2011: pages 1291–1321, ISSN 0022-5096.

[21] Li, C.; Der Kiureghian, A.: Optimal Discretization of Random Fields. *Journal of Engineering Mechanics Division ASCE*, volume 119, nr. 6, 1993: pages 1136–1154, ISSN 0733-9399.

[22] Schlangen, E.; Garboczi, E.: Fracture simulations of concrete using lattice models: Computational aspects. *Engineering Fracture Mechanics*, volume 57, nr. 2-3, 1997: pages 319–332, ISSN 0013-7944.

[23] van Mier, J.: *Concrete Fracture: A Multiscale Approach*. CRC Press, October 2013, ISBN 9781466554702.

[24] Vořechovský, M.: Simulation of simply cross correlated random fields by series expansion methods. *Structural safety (Elsevier)*, volume 30, nr. 4, 2008: pages 337–363, ISSN 0167-4730.

[25] Vořechovský, M.; Sadílek, V.: Computational modeling of size effects in concrete specimens under uniaxial tension. *International Journal of Fracture*, volume 154, nr. 1-2, 2008: pages 27–49, ISSN 0376-9429.

Ing. Jana Kaděrová

Vysoké učení technické v Brně
Fakulta stavební
Ústav stavební mechaniky

Jana.Kaderova@vutbr.cz

Vzdělání

od 2/2012   **Vysoké učení technické v Brně, Fakulta stavební**

- doktorský studijní program, obor: Konstrukce a dopravní stavby, Ústav stavební mechaniky
- Téma dizertace: Stochastická mechanika, vedoucí: doc. Ing. Jan Eliáš, Ph.D., Státní zkouška složena dne: 1. 10. 2014

6/2005 – 1/2012   **Vysoké učení technické v Brně, Fakulta stavební**

- obor: Konstrukce a dopravní stavby (bakalářský a navazující magisterský studijní program)
- Téma diplomové práce: „Multi-filament yarns testing for textile-reinforced concrete", vedoucí: prof. Ing. M. Vořechovský, Ph.D., prospěla s vyznamenáním
- Téma bakalářské práce: „Testování statistického vlivu velikosti pomocí čtyřbodového ohybu", vedoucí: prof. Ing. M. Vořechovský, Ph.D., prospěla s vyznamenáním

6/1997 – 5/2005   **Gymnázium Havířov, ul. Komenského**

- všeobecné osmileté gymnázium

Odborná praxe

od 2017   **Produktový inženýr v IDEA StatiCa s.r.o.**

- odborná podpora uživatelů, zaškolování, tvorba dokumentace, testování softwaru, reprezentace firmy na odborných akcích

2012 – 2016   **Asistent na Ústavu stavební mechaniky, VUT v Brně, Fakulta stavební**

- výuka odborných předmětů (Základny stavební mechaniky, Statika I, Statika II)
- řešení a spolupráce na vědeckých projektech zaměřených na numerické simulace porušování betonu – lomová mechanika
- překlad skript do angličtiny pro předmět Pružnost a pevnost
- tvorba řešených příkladů do předmětu Pružnost a pevnost
- pomoc v laboratorní zkušebně Ústavu stavební mechaniky

Zahraniční pobyty a odborné kurzy

7/2014	**BOKU Wien, Rakousko** kurz „Multi-Scale and Multi-Phase Modeling of Aging Concrete Structures"
6/2014	**RWTH Aachen, Německo** Erasmus Training
3 – 8/2013	**RWTH Aachen, Německo** Erasmus stáž na Lehrstuhl und Institut für Massivbau
8/2012	**Bauhaus Summer School, Weimar, Německo** dvoutýdenní kurz „Model Validation and Simulation"
5/2012	**Akademie věd ČR, Brno** Kurz základů vědecké práce
7/2009 – 6/2010	**Technical University of Denmark, Lyngby, Dánsko** dvousemestrální Erasmus studijní pobyt – civil engineering

Ocenění

2/2012	Uznání děkana Fakulty stavební VUT v Brně za vynikající studijní výsledky a za vzorně vypracovanou bakalářskou práci a její obhajobu¨
6/2009	Cena rektora VUT v Brně za vynikající studijní výsledky a další aktivity po celou dobu studia
	Uznání děkana Fakulty stavební VUT v Brně za vynikající studijní výsledky a za vzorně vypracovanou bakalářskou práci a její obhajobu
5/2009	1. Místo ve fakultním kole SVOČ (Stavební mechanika), účast v mezinárodním kole (Bratislava, Slovensko)

Počítačové znalosti

Matematické	Matlab, Maple, Gnuplot, Python
Inženýrské	Scia Engineer, Nexis, Atena, FReET, InRoads, RailCAD, ARAMIS, IDEA StatiCa
Textové	MS Office, LaTeX
Grafické	AutoCAD, CorelDRAW, Flash

Znalost cizích jazyků

Angličtina	úroveň C1, Státní jazyková zkouška základní (5/2004)
Němčina	úroveň B2

Ostatní

Řidičský průkaz	skupina B
ADRA	dobrovolnice v domově pro seniory (2016 – 2017)
Člověk v tísni	dobrovolná pomoc lidem zasaženým povodní (2010)
Česká tábornická unie	pomoc na dětských letních táborech (2009 – 2012)

Abstract

The thesis presents results of a numerical study on the performance of 3D discrete meso–scale lattice–particle model of concrete. The existing model was extended by introducing the spatial variability of chosen material parameter in form of random field. An experimental data from bending tests on notched and unnotched beams was exploited for the identification of model parameters as well as for the subsequent validation of its performance. With the basic and the extended randomized version of the model, numerical simulations were calculated so that the influence of the rate of fluctuation of the random field (governed by the correlation length) could be observed. The final part of the thesis describes the region in the beam active during the test in which the most of the fracture energy is released in terms of its size and shape. This region defines the strength of the whole member and as shown in the thesis, it does not have a constant size but it is influenced by the geometrical setup and the correlation length of the random field.

Key words
Concrete, discrete model, meso-scale, lattice-particle model, probability, random field, experiments, crack, active zone, fracture energy

Abstrakt

Dizertační práce představuje výsledky numerické studie provedené s pomocí 3D diskrétního mezo-úrovňového mřížkově-částicového (lattice-particle) modelu betonu. Již existující model byl rozšířen o prostorovou variabilitu některých materiálových parametrů pomocí náhodného pole. Laboratorní experimenty z literatury posloužily jednak k identifikaci parametrů, zároveň také umožnily ověřit správné chování modelu s určenými parametry. Se základním i rozšířeným modelem byla provedena série numerických simulací zaměřená na popis vlivu míry proměnlivosti náhodného pole definované korelační délkou na celkovou únosnost prvku. Závěr práce je věnován popisu oblasti, ve které je během zatěžování uvolněna většina lomové energie, a to z hlediska její velikosti i tvaru. Tato zóna rozhoduje o celkové pevnosti prvku a jak je ukázáno, její tvar i velikost nejsou konstantní, ale závisí na typu zatěžování (přítomnost zářezu) a také na korelační délce náhodného pole.

Klíčová slova
Beton, diskrétní model, mezo-úroveň, mřížkově-částicový model, pravděpodobnost, náhodné pole, experiment, trhlina, aktivní zóna, lomová energie